A fast approach to measuring the thickness uniformity of a homoepilayer grown on to any type of silicon wafer

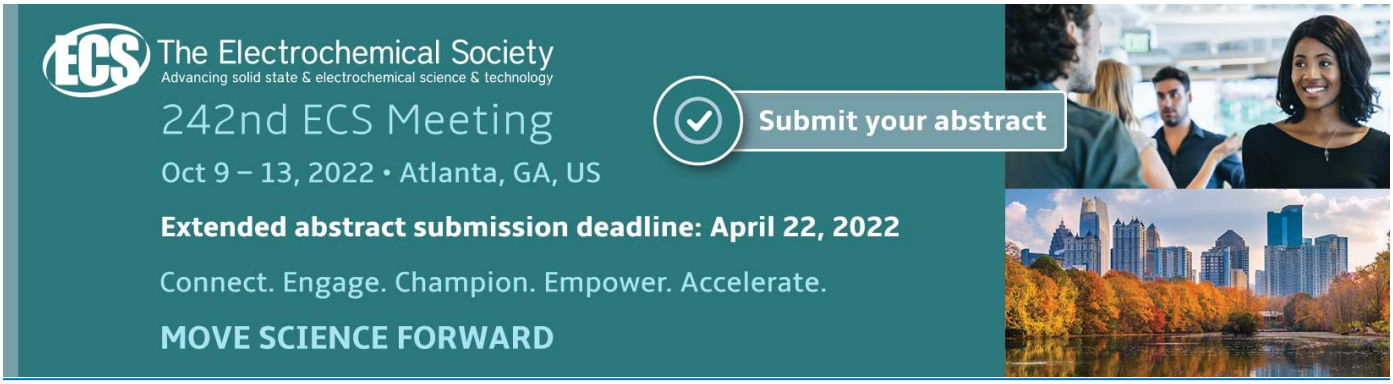

OPEN ACCESS
IOP Publishing
Semiconductor Science and Technology
Semicond. Sci. Technol. **37** (2022) 065003 (11pp)
https://doi.org/10.1088/1361-6641/ac5f69

A fast approach to measuring the thickness uniformity of a homoepilayer grown on to any type of silicon wafer

Maksym Myronov*, **Gerard Colston, Jack Davies and Laura Michael**

Department of Physics, The University of Warwick, Coventry CV4 7AL, United Kingdom

E-mail: M.Myronov@warwick.ac.uk

Received 24 November 2021, revised 14 January 2022
Accepted for publication 21 March 2022
Published 20 April 2022

Abstract

Optical reflection spectroscopy techniques offer a non-destructive and fast method of measuring the thickness of silicon (Si) epilayers, enabling very fast thickness uniformity mapping across the full surface of epiwafers up to 450 mm in diameter. However, their use for undoped or low doped epilayers has traditionally been constrained by a dependence on high levels of substitutional doping in the Si wafer, at values of approximately 5×10^{19} cm^{-3}. Whilst the high dopant concentration of this wafer creates the necessary reflectance boundary for optical reflection, their commercial availability is mainly limited to the (001) surface orientation only. Optical reflectance techniques are therefore also limited in use to this orientation. In this article, an approach to measure the thickness of a Si epilayer on any Si wafer, independent of its crystallographic orientation, doping type and value, using Fourier transform infrared reflection spectroscopy is proposed and demonstrated. Because the use of non-destructive optical reflection spectroscopy is already common and well-understood within both industry and academia, this technique could easily be implemented within existing industrial and research fabrication facilities. Furthermore, this approach could be adapted, with further work, to suit other semiconductor materials and other optical reflection techniques.

Keywords: silicon, epitaxy, FTIR, reflectance

(Some figures may appear in colour only in the online journal)

1. Introduction

The epitaxial growth of epiwafers forms the backbone of the entire semiconductor industry, whose global sales were worth approximately $439 billion in 2020 alone [1]. This is because the technology underpins the production of all microelectronic solid-state devices, without which none of the computerised or radio-based technology, so heavily relied upon in the modern world, could operate. Today, the semiconductor industry demands the fabrication of increasingly complex epiwafer structures, with specifically tailored electrical and optical properties to fit a variety of new applications. Producing these not only requires improvements to epiwafer fabrication, but also to the characterisation techniques used to analyse the results.

In an epitaxial process, crystal epilayers are grown on to an underlying 'seed' crystal (called a substrate or wafer) to form an epiwafer using deposition processes such as chemical vapour deposition (CVD) and molecular beam epitaxy [2]. This is referred to as homoepitaxy when the epilayer and wafer material match (regardless of differing concentrations of impurity or doping elements), and heteroepitaxy when they differ. Whilst the crystal orientation of the epilayers is fixed by the wafer, it is the other epilayer properties that control the type

* Author to whom any correspondence should be addressed.

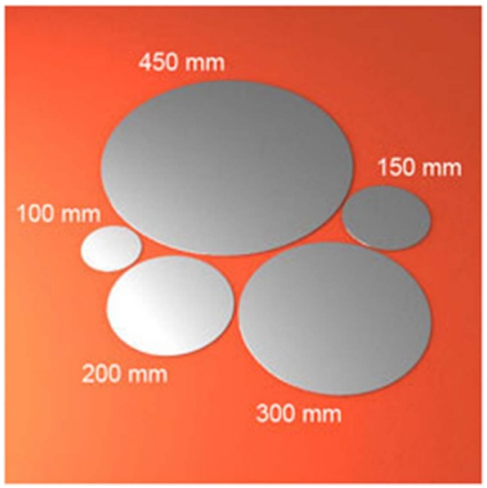

Figure 1. Si wafers varied in diameter between 100 and 450 mm.

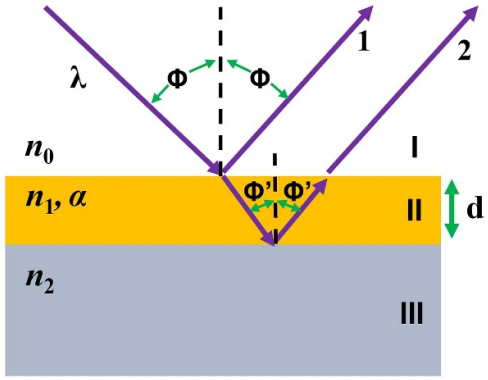

Figure 2. Radiation reflecting off a thin film epiwafer, resulting in two interfering beams 1 and 2 (reflected from interfaces I/II and II/III respectively). The arbitrary angle of incidence Φ is only included for clarity. In specular reflection, the beam is at normal incidence (i.e. $\Phi = \Phi' = 0$).

of device that is produced from the final epiwafer. Their number, atomic composition, and order of growth are what determine an epiwafer's precise structural, electronic and optical properties; whilst quality and performance are determined by the epilayer's purity, structural perfection and individual layer homogeneity. By precisely controlling these epilayer properties, state-of-the-art semiconductor devices can be fabricated to fit a variety of different purposes.

Of particular importance to epitaxial growth in the semiconductor industry is silicon (Si). In addition to its abundance, this element can be refined to exceptional levels of quality and purity using either Czochralski crystal pulling or free float zoning [3]. The latter point making it essential to industries involved in the fabrication of integrated circuits. The extent of Si research has also led to dramatic advancements in the standard size of a Si wafer, from the 100 mm diameter first introduced into mass production in late 1975, to the current Si industry standard of 300 mm that began manufacture in 2001, see figure 1. The larger diameter means a single Si wafer can produce more semiconductor devices, greatly improving productivity and enabling cost reductions. For example, an increase in diameter from 200 to 300 mm enables 2.25 times more identically sized microchips to be obtained from a single epiwafer. It is for these reasons that Si is now incorporated into the manufacture of 99% of all semiconductor devices (either as the wafer or the material used to grow the epilayers), and why total Si wafer demand is expected to reach over 120 million 300 mm wafer equivalents in 2021 [1]. The epiwafers produced from these will form the essential components of almost every electronic, optoelectronic and radio-controlled device on the planet.

As is clear from the above, epitaxial growth is central to semiconductor device fabrication, but it is not sufficient for this purpose on its own. It must also be possible to analyse the grown epiwafer structures, to determine whether they have the desired properties for the intended use. Without the numerous characterisation techniques that have been developed to do this, it would be impossible to produce semiconductor devices of any real purity or quality. Of particular importance in this investigation are the techniques used to explore epilayer thickness uniformity. This plays a role in determining the consistency of electrical and optical properties across an epiwafer, which must both remain uniform to maximise the available epiwafer surface suitable for device fabrication. In addition, full-wafer thickness characterisation of epitaxially grown thin films is used to calibrate the gas flow and temperature offsets of an epitaxial reactor during set up and after maintenance, which is important for optimising the reactors output. For these reasons, fast and reliable homoepitaxial thin film thickness characterisation techniques capable of measuring uniformity across the full surface of an epiwafer are essential to maintaining high industrial yield.

Several non-destructive techniques (so called as the analysis incurs no damage to the epiwafer) are available to measure homoepitaxial thin film thicknesses. Ellipsometry, for example, exploits phase information between two reflection boundaries to determine optical constants, from which the thickness can be determined [4]. Another possibility is x-ray reflectivity (XRR), which uses the total reflection from a surface at a series of wavelengths to directly measure layer thicknesses of up to ∼150 nm. Both of these techniques deliver accurate results, but are slow in their acquisition and/or analysis of data. This presents a problem when taking multiple readings of an epiwafer's surface to build a thickness contour map, as each measurement extrapolates the length of this delay to the point that both techniques become burdensome.

A third technique that avoids this pitfall is Fourier transform infrared (FTIR) spectroscopy, which uses the Fourier relationship between an interferogram and the electromagnetic spectrum of a detected probe beam to return information about a sample the beam has interacted with. It is the specific nature of the beam/sample interaction that determines the sample information that can be obtained, and to determine thickness requires the probe beam to be reflected off both the top and bottom of an epilayer prior to analysis, see figure 2. The constructive/destructive interference of these beams at the detector creates periodic oscillations in the resulting interferogram, shown in figure 3, and it is the period of these that

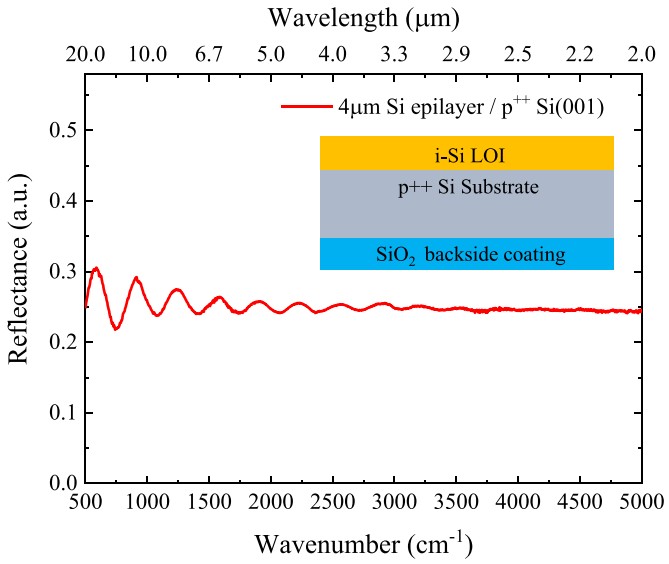

Figure 3. Example of FTIR reflectance spectrum. It shows oscillating reflectance caused by the constructive and destructive interference of two beams reflected off the insert epiwafer structure, consisting of the intrinsic 4 μm thick Si (i-Si) epilayer grown on heavily boron doped p^{++} Si(001) substrate.

determines the epilayer's thickness. This is known as FTIR reflection spectroscopy.

To ensure that light is reflected off both the top and bottom of an epilayer, the epilayer/wafer directly below (material III in figure 2) needs to meet certain criteria. First and foremost, there must be a sufficient difference in the (complex) refractive indices of the two layers to create a reflection boundary at their interface. Whilst such a difference arises naturally at the vacuum/epilayer interface (I/II), it is more difficult to create at the homoepitaxial inter-epilayer boundary (II/III). This is because changing the refractive index of layer II (or III) often relies on changing the layer's structure, causing strain energy to build up at the interface with layer III (or II). When growing such a structure, this strain energy can cause defects to form at the interface (above a critical thickness), ruining the uniformity of the epilayer and altering the epiwafers properties. For this reason, the refractive index of material III needs to be altered so that it is different to what is subsequently grown on top, but its structural properties must remain the same. In addition to this requirement, it is also important that all light transmitted into material III be scattered so as not to cause additional interference upon any subsequent reflection. This means material III must have a high absorption coefficient (α) to scatter (absorb) the radiation, as well as a sufficient thickness to ensure complete absorption. In the interest of efficiency, an optimum combination of both parameters is important.

The current standard approach taken in FTIR reflection spectroscopy is to grow the Si thin film layer of interest (LOI) onto a heavily doped wafer (corresponding to a doping concentration greater than 5×10^{19} cm^{-3}, and a resistivity of less than 0.025 Ω cm [5]). The incorporation of high concentrations of group 3/5 impurities into the wafer (doping) causes a shift in the refractive index, creating the necessary reflectance at the interface without significantly altering the lattice constant. The high doping concentration also increases the absorption coefficient, so that transmitted light is absorbed quickly.

Whilst this method does create the necessary conditions for FTIR reflection spectroscopy however, it also has several drawbacks. The production of heavily doped wafers is difficult in comparison to other wafer types. The very high level of doping that needs to be incorporated into the bulk crystal is challenging and typically results in the appearance of: point defects, dopant clusters and poor uniformity across large diameter wafers. As a result, only heavily doped wafers of the standard (001) orientation are commercially available, creating obvious difficulties for research on more exotic orientations. Another problem with heavily doped wafers is the doping itself. During higher temperature deposition processes, particularly those involving chloride precursors, some of the doping material in the wafer can evaporate from the underside and cause unwanted impurity incorporation in the growing LOI and any future epitaxial layer within the growth system. To reduce this, each heavily doped wafer must be 'back-sealed' with a thin silicon dioxide SiO_2 layer, further increasing the cost and complexity of their production. With these difficulties in mind, it is the aim of this research to find an alternative approach to thickness characterisation using FTIR reflection spectroscopy that can negate the requirement of the heavily doped Si wafer.

2. A novel approach

Instead of the use of heavily doped Si wafers to create the reflective boundary beneath the LOI, this work proposes that a heavily-boron-doped epilayer (B:Si) could be grown on to a wafer as an intermediate layer, before the LOI is grown on top (shown schematically in figure 4). This overcomes the problems encountered with heavily doped wafers and could be applicable to a Si wafer of any crystallographic orientation, off-cut, doping type and value. It could also be adapted and applied to other non-Si materials like germanium (Ge), silicon carbide (SiC), gallium arsenide (GaAs), etc.

The choice of group 3 boron (B) over alternative options, such as the group 5 elements phosphorous (P), arsenic (As) and antimony (Sb), was made for several reasons. The first is the relative reluctance of other elements to incorporate into the lattice during epitaxy of a thin film at high doping concentrations, i.e. $\geqslant 5 \times 10^{19}$ cm^{-3}. This leads to segregation and clustering, imposing a low limit on the critical thickness of the layer able to be grown defect-free. Above this critical thickness a large number of dislocations form, decreasing the surface uniformity and disrupting electrical properties, such that the epiwafer can no longer be used for device production [6]. Furthermore, the lack of incorporation would also lead to diffusion and/or segregation of impurity atoms into the LOI as it is subsequently grown on top of the heavily doped layer. As reflection spectroscopy requires a sharp change in the refractive index at the boundary, this 'smearing' of the dopant could cause issues in modelling of the resultant reflection spectrum.

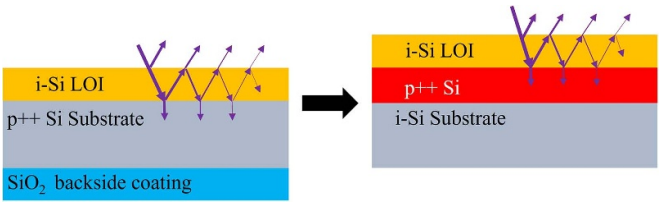

Figure 4. Current (left) and proposed (right) epiwafer approaches to FTIR reflection spectroscopy.

B has been found to have a lower diffusivity in Si than As, P and Sb [7], and as such represents a better choice.

The viability of $Si_{1-x}Ge_x$ and $Si_{1-y}C_y$ epitaxial binary alloys was also considered, however these are even more problematic. In the former case, the required Ge concentration for an adequate reflection boundary corresponds to a very low critical thickness, such that insufficient absorption would occur within the $Si_{1-x}Ge_x$ epilayer. Similarly, it has been reported [8] that defect free $Si_{1-y}C_y$ epilayers are only achievable for thicknesses of tens of nanometres, even with a carbon (C) content of a few per cent. This causes both insufficient reflectance and absorption, implying it is wholly unsuitable for the approach proposed here.

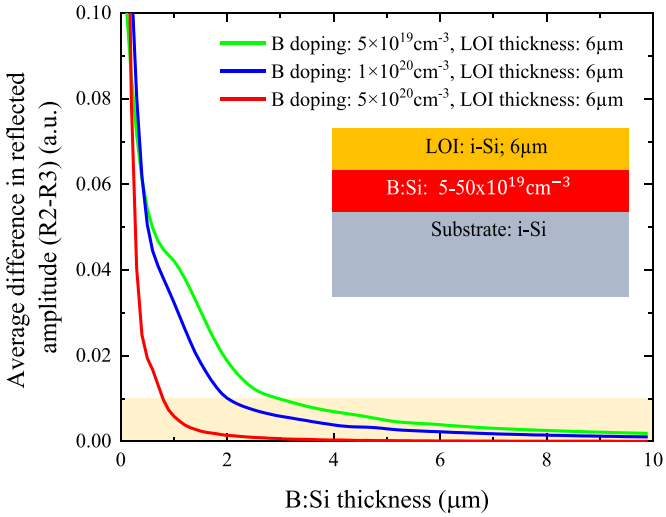

Figure 5. Simulated predictions of the difference between the R3 and R2 reflectance when a 2–20 μm probe beam is incident on the epiwafer structure shown in the insert. The B:Si epilayer doping was varied whilst the thickness was kept constant at 6 μm. Specifically, doping concentrations of 5×10^{19} cm^{-3}, 1×10^{20} cm^{-3}, and 5×10^{20} cm^{-3} were studied. The yellow area represents what was considered an acceptable level of difference in the R3 and R2 reflectance for FTIR reflection spectroscopy.

3. Simulation

Prior to experimental investigation, simulations were developed to estimate the thickness and doping concentration that the proposed B-doped epilayer would require for FTIR reflection spectroscopy to accurately measure the thickness of a LOI in the spectrum range of 2–20 μm. This was done by simulating the interferogram that would be generated if a probe beam were reflected off the proposed epiwafer structure (right of figure 4), using models to determine the changes that the above parameters have on the epilayers optical properties and reflection boundaries. The relationship between the complex refractive index (**n**) of doped Si and the concentration of B dopant was modelled using the Drude model [9]. The real part of **n** being the normal refractive index (n), and the imaginary part being the extinction coefficient (κ) that can be used to determine the absorption coefficient (α). As part of this model, an empirically derived equation of mobility specifically tailored to group 3 dopants [10] was used. Advantage was also taken of the fact that both the normal refractive index and extinction coefficient of undoped Si remain constant across the 2–20 μm spectrum range, at values of $n = 3.43$ and $\kappa = 0$ respectively [11]. To then model the reflection of the probe beam, complex Fresnel equations were derived via an extension of the method in [12]. These were used to find the total reflectance resulting from one (R1), two (R2) and three (R3) reflection boundaries of the proposed epiwafer structure. Note that notation shall be used where R1 encompasses only the light reflected from the first (air/LOI) boundary, R2 refers to the light from both the first and second (LOI/B:Si) boundaries, and R3 represents the total reflected light for all three boundaries (including the third B:Si/Si wafer boundary).

Using the above models, a simulation involving the R2 reflectance formula was developed to first find the threshold doping concentration sufficient to create the inter-layer (LOI/B:Si) reflection boundary necessary for FTIR reflection spectroscopy. After determining this to be 5×10^{19} cm^{-3}, the total difference in reflectance between R3 and R2 was then modelled to isolate and study the absorption in the B-doped epilayer. By plotting this against the thickness of the B-doped epilayer for varying values of B concentration, an optimum combination of the two could be determined. Specifically, a combination that maximises the thickness resolution of the FTIR spectrometer, whilst minimising the dopant and thickness that the epilayer requires. An example of this analysis for three different doping concentrations is shown in figure 5, these being 5×10^{19} cm^{-3}, 1×10^{20} cm^{-3} and 5×10^{19} cm^{-3} respectively. This result suggests that a B-doped epilayer of 5 μm thickness would be sufficient for FTIR reflection spectroscopy if the minimum doping concentration of 5×10^{19} cm^{-3} were used. Equivalently though, it also suggests that a lower thickness could be used instead, provided the doping concentration was increased appropriately. For example, at a doping concentration of 5×10^{20} cm^{-3}, a 1 μm thickness should result in accurate thickness measurements via the proposed approach. The results of these simulations were used as guidance when fabricating the experimental epiwafers.

4. Experimental techniques

4.1. Epitaxial growth

All epiwafers used in this investigation were grown on to 200 mm Si(001) wafers in an ASM Epsilon 2000 CVD reactor,

within a temperature range of 800 °C–1150 °C. At these temperatures the Si epilayer's growth rate could be varied between ∼0.1 and 20 nm s^{-1} for the same growth conditions, allowing thick epilayers to be grown in reasonable times. A dichlorosilane precursor, mixed with a hydrogen carrier gas, provided the source of Si in the epilayers, but alternative choices such as trichlorosilane, silane, disilane and trisilane would have worked equally well. When required, diborane was also added to the gas stream to produce the B-doped epilayers.

4.2. Thickness measurements

The experimental reflectance spectra were produced using the Bruker VERTEX 70 V FTIR spectrometer, with an attachment suitable for specular reflectance measurements of 200 mm diameter wafers. This equipment has a standard resolution of 0.4 cm^{-1} [13] and uses a mid-IR radiation source capable of producing spectrums within the 2–20 μm range. Alternatively, this can be expressed as either an energy range (0.62–0.062 eV) or a wavenumber range (5000–500 cm^{-1}). To model the experimental spectra and produce thickness results, associated 'SCOUT' software was then used. Overall, this can accurately measure and analyse single Si epilayer thicknesses of 0.5 μm or greater, a limit imposed by the spectrum fitting algorithm which requires at least one full oscillation in the spectrum to make an accurate fit [14].

In addition to single point measurements, the reflectance attachment is also able to automatically reposition it is point of measurement on an epiwafer's surface and perform multiple thickness measurements in a single sequence. The locations of these points are fully programmable using pre-programmed templates, and the results can be used to plot an accurate thickness contour map of the epiwafer. This is important in determining the thickness uniformity of an epilayer, the extent of which is often denoted using one of two parameters: the uniformity given by:

$$\text{Uniformity}\,(\%) = \frac{(x_{\max} - x_{\min})}{(x_{\max} + x_{\min})} \times 100, \tag{1}$$

where x represents the measured thicknesses, and the standard deviation of the measured thicknesses divided by the mean (σ/mean), given by:

$$\frac{\sigma}{\text{mean}} = \frac{\sqrt{\frac{\Sigma(x_i - \text{mean})^2}{N}}}{\text{mean}} \tag{2}$$

where x_i is each measured data point and N the total number of points. It should be noted that these parameters can also be applied to four-point probe (4PP) resistivity uniformity measurements and analysis, see the next section 4.3.

4.3. Resistivity measurements

To accurately determine an epilayers doping concentration, a collinear 4PP, with 1 mm inter-probe spacing, was used to first find its electrical resistivity, which could then be converted into the layers corresponding active impurity concentration. Provided the surface region being characterised is a few mm from the wafers edge, this equipment is capable of measuring sheet resistivity as high as $10^{10}\,\Omega\ sq^{-1}$ and as low as $10^{-6}\,\Omega\ sq^{-1}$ (for suitably small or high currents respectively) [4]. However, there are errors associated with both resistive heating and current leakage that had to be considered. The effect of the former was found to be negligible as all the epilayers characterised in this way had a high doping concentration, and so the current required was relatively small. To mitigate the latter, all B:Si epilayers used in this research were grown onto lightly n-doped (1×10^{15} cm^{-3}) Si(001) wafers. Due to the resultant formation of a p–n junction between the p^{++}-Si epilayer and the n^- Si wafer, a depletion region was created at the boundary which minimised leakage current. Note, however, that the doping concentration in these is not sufficient to affect the results of FTIR reflection spectroscopy.

4.4. Crystal structure

High levels of B dopants within Si have been shown to reduce the lattice structure of the B:Si material when reaching alloy levels of composition (>1% or $\sim 5 \times 10^{20}$ cm^{-3}). As discussed in sections 1 and 2, these heavily doped B:Si epilayers have a low critical thickness and exceeding this will lead to relaxation and potential defect formation which may impact the growth of any subsequent epilayers. Ω–2θ coupled scans were obtained through x-ray diffraction (XRD) from a Panalytical X'Pert MRD diffractometer using Cu Kα1 radiation to assess the impact of B incorporation on the lattice structure of the B:Si epilayer.

4.5. Surface morphology

The formation of defects within the Si epilayers is unwanted and will result in non-ideal surface morphology. Atomic force microscopy (AFM) was utilised to ensure the surface of the B:Si epilayers and subsequently grown i-Si LOI were free from any such defects. These AFM scans were obtained using a Bruker Icon operating in ScanAsyst mode.

5. Results and discussions

Using predictions from the simulated data, a series of epiwafers were grown on to lightly n-doped Si(001) wafers with the intent of experimentally verifying the proposed approach to FTIR reflection spectroscopy. These epiwafers can be split in to the two general structures shown in figure 6, hereafter labelled structure A and structure B. Structure A epiwafers were grown first and consist of a B-doped epilayer grown on a lightly doped n-Si wafer. These were used to study the effects of high doping concentrations on the structure of the B-doped epilayer, as well as to fine-tune the thickness and doping concentration parameters estimated using the simulations. Structure B epiwafers were grown after considering the results of the structure A analysis. These also have a B-doped epilayer grown onto the lightly doped wafer, but in this case an additional epilayer of undoped Si was then grown on top. The purpose of this additional layer was to simulate a LOI that can be characterised using FTIR reflection spectroscopy in the

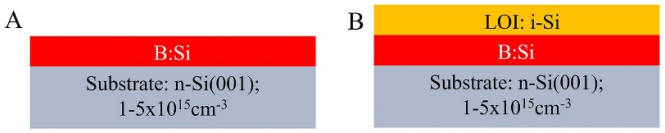

Figure 6. The two experimentally grown epiwafer structures: one with only a B doped Si epilayer grown ((A), left), and the other with the additional inclusion of a LOI ((B), right).

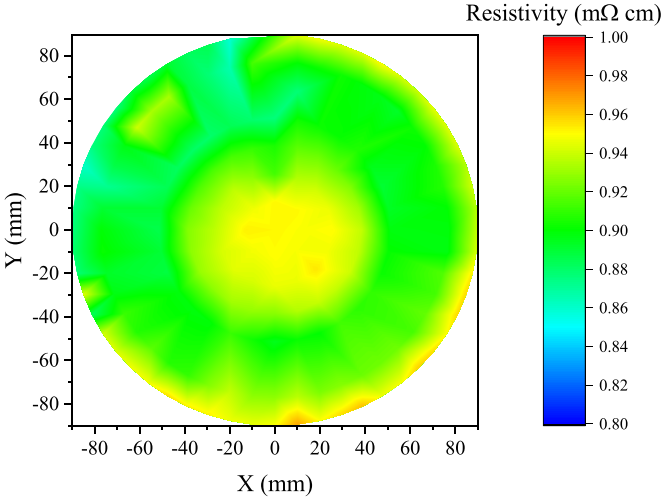

Figure 7. The 4PP resistivity map of a 10 μm B doped Si epilayer with SD/mean of 2.9%. The B concentration is estimated to be $\sim 5 \times 10^{20}$ cm^{-3}.

approach proposed in this research. In this way, it was possible to experimentally validate this approach.

The simulated results suggested that a doping concentration of at least 5×10^{19} cm^{-3} would be required in the B-doped epilayer to create a sufficient reflectance boundary for FTIR reflection spectroscopy. Incorporating such high doping concentrations into epitaxially grown layers is difficult, and it was first necessary to ensure that the dopant would be evenly distributed throughout the grown epilayers. To do this, a 10 μm thick B-doped epilayer was grown on to a 200 mm diameter lightly doped n-Si(001) wafer, with a doping concentration of approximately 5×10^{20} cm^{-3}. This being an example of a structure A epiwafer as previously defined. A resistivity contour map of this epiwafer was then produced using 4PP characterisation, figure 7, which showed an excellent SD/mean of 2.9%. From this, it was concluded that it was possible to produce uniform doping even at concentrations ten times as high as what is expected to be required.

It was also important to study the effect of these high doping concentrations on the structure of the epilayer, to determine whether a LOI could be grown on top without the formation of large-scale defects. Figure 8 shows high resolution x-ray diffraction (HR-XRD) coupled scans obtained from three epiwafers with different B doping levels in the 2 μm thick B:Si epilayer, i.e. 6×10^{19} cm^{-3}, 5×10^{20} cm^{-3} and 1×10^{21} cm^{-3}. The peak shared by all three of these epiwafers at the $\sim$34.56° mark is from the lattice structure of the Si wafer, as would be expected. However, additional peaks can

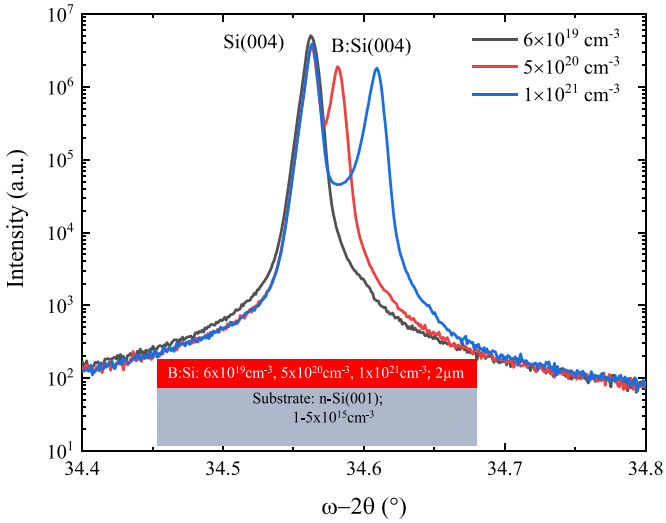

Figure 8. XRD coupled scans of 2 μm thick Si epilayers doped with varying levels of B. The appearance of the $Si_{1-x}B_x(004)$ diffraction peak shows that alloy levels of B incorporation have been achieved and relaxation is likely to occur.

also be seen for the two higher doped epilayers (5×10^{20} cm^{-3} and 1×10^{21} cm^{-3}), with the epilayer containing the highest concentration of the three resulting in the largest separation from the shared Si wafer's peak. These secondary peaks result from the silicon–boron alloy that has formed in the B-doped epilayer because of the incredibly high doping concentrations, and were identified as coming specifically from the B:Si(004) reflection plane. In addition to providing further evidence of uniform dopant incorporation at high concentrations, the clarity of the peaks also suggests that the B:Si epilayers are under tensile biaxial strain to remain matched to the Si wafer underneath. As mentioned in section 1, any relaxation within the B:Si epilayers would lead to defect formation and surface roughening, which would make the epilayers unsuitable for subsequent epitaxy on top. Because the peaks remain so defined here however, figure 8 suggests that B doping concentrations of even 1×10^{21} cm^{-3} are achievable without epilayer relaxation for thicknesses of at least 2 μm.

This was further evidenced by the surface mappings obtained of these epiwafers using AFM, an example of which is shown in figure 9. Each of the epilayers was found to be smooth with an RMS surface roughness of below 200 pm. The smooth surface, and absence of any crosshatch pattern, implies the B:Si epilayer is fully strained. Otherwise, surface roughening would occur due to strain relaxation in the tensile strained epilayer. As a result, this suggests that no defect formation occurs within the B:Si epilayers even at the highest analysed concentration of 1×10^{21} cm^{-3}. Therefore, these B:Si epilayers are suitable as platforms for further epitaxial growth of the LOI.

Having established that the highly B-doped Si epilayers analysed above are both uniformly doped and capable of supporting further epitaxial growth, the next task was to fine tune the optimum B-concentration and thickness parameters first estimated via simulation. As was discussed in section 1, the

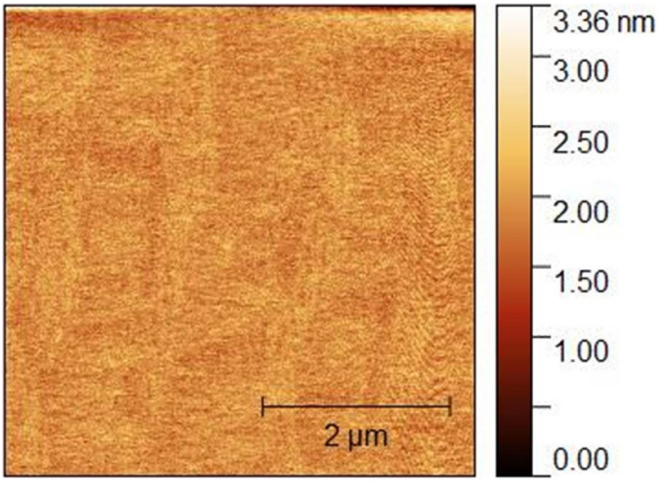

Figure 9. The 5 × 5 μm scan of a 10 μm thick B:Si epilayer with ∼5 × 10^{20} cm^{-3} dopant incorporation. The result shows a RMS roughness of <200 pm.

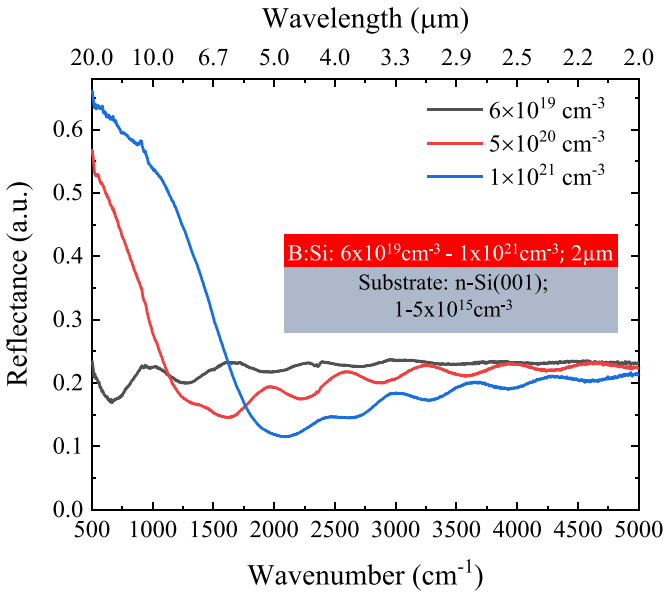

Figure 10. Reflectance spectra for 2 μm thick B:Si epilayers of varying B-concentration.

ideal B-doped epilayer for FTIR reflection spectroscopy will have a strong reflection boundary at the LOI/B:Si interface, and absorb all light that is transmitted into it. As was demonstrated via the simulations, these two criteria were isolated and studied separately to determine the optimum B-doped parameters. First by determining the doping concentration required to create a sufficient reflection boundary, and then finding the thickness that an epilayer doped to this concentration required to absorb all transmitted light from the 2–20 μm probe beam. The coded simulation predicted that a minimum doping concentration of 5 × 10^{19} cm^{-3} would be required for this, and went on to suggest that the strength of the boundary would then continue to increase (on average across the 2–20 μm mid-IR spectrum measured) at higher concentrations. To test this, a series of structure A epiwafers were grown, all using higher doping concentrations than the simulated minimum, and analysed using FTIR reflection spectroscopy. The results of this are shown in figure 10.

From these results, it can be observed that increasing the doping concentration has three separate effects on the detected spectra. These are a decrease in the reflected intensity, a shift of the 'shoulder' seen on the left-hand side of the figure to higher wavenumbers, and an increase in the strength and clarity of the spectrum oscillations. The first of these phenomena is a result of the increase in absorption that occurs at the B:Si/Si wafer interface with increasing doping concentration in the B:Si epilayer, resulting in less light from the incident probe beam returning to the FTIR detector. This effect is only observed because structure A epiwafers are being used, and will not be present in the proposed structure B epiwafers. The second observation is because the 'shoulder' is a direct result of the B-doped Si epilayer's plasma frequency. This is defined as the value at which the real part of the permittivity of a material is equal to zero [9], explaining the observed sharp rise in reflectance. Moreover, because the plasma frequency is proportional to the square-root of the electrically active doping, the shoulder will shift to higher wavenumbers as the doping is increased if the B atoms occupy substitutional sites in the Si lattice structure. As this is exactly what is observed, it provides further evidence of successful lattice incorporation of the B-dopant even at very high doping concentrations. The third and final effect is a result of the higher B doping concentrations causing larger changes in the refractive index of the B:Si epilayer, and therefore stronger reflectance at the B:Si epilayer/Si wafer interface. The interference between light reflected from the top and bottom of the epilayer respectively is thus increased, leading to stronger oscillations.

In order to determine the optimum doping concentration, it was necessary to balance the latter two of these factors. This was because the epiwafers with higher B doping concentrations show stronger and more defined oscillations, increasing the accuracy of the thickness measurement. But conversely, the shoulder on these results obscures more of the spectrum, which decreases the wavenumber range available for characterisation. After due consideration, it was determined that the optimum value must be 5 × 10^{20} cm^{-3}.

Having ascertained the ideal B:Si doping concentration, the impact of B:Si alloy thickness was then investigated to determine the ideal structure for complete absorption of light within the B:Si epilayer. This was once again done using three structure A epiwafers, where the doping concentration in the B-doped epilayer was fixed at 5 × 10^{20} cm^{-3} and the thickness was grown to 2, 6 and 10 μm respectively. The result of FTIR characterisation on these epiwafers is shown in figure 11. When there is complete absorption in a structure A epiwafer, all light transmitted into the B:Si epilayer will have been scattered such that none arrives at the detector. Accordingly, the desired epilayer will produce a spectrum with none of the characteristic oscillations seen in figure 10. The results show that as the thickness of the B:Si epilayer increases the amplitude of secondary oscillations in the reflectance spectra decrease, and at 10 μm become negligible. The obvious reason

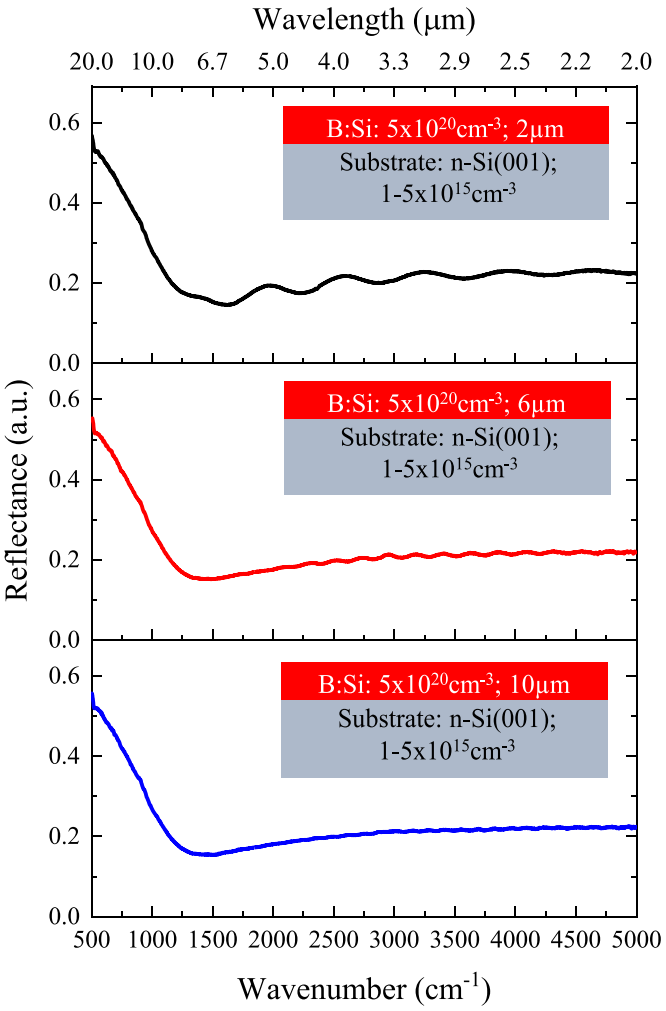

Figure 11. Reflectance spectra for B:Si epilayers of varying thickness, with a fixed doping of 5×10^{20} cm^{-3}. Reflectance data has been shifted to separate the spectra for clarity.

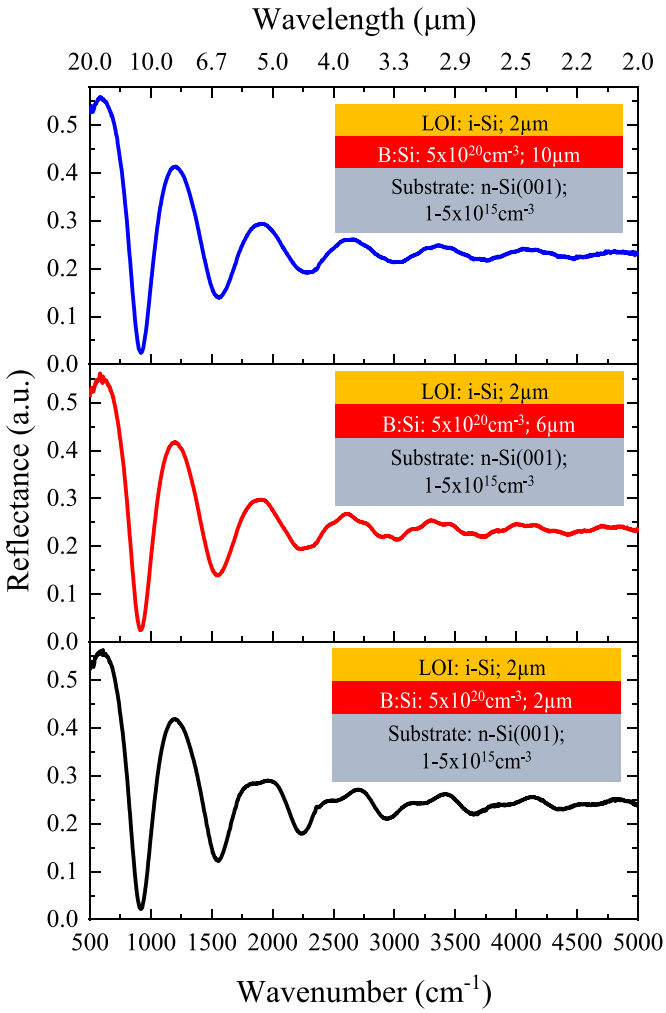

Figure 12. Reflectance spectra for undoped Si epilayers of 2 μm thickness, grown upon varying thickness B:Si platforms with doping concentrations of 5×10^{20} cm^{-3}. Reflectance data has been shifted to separate spectra for clarity.

for this being that the increasing amounts of material through which the IR light must travel means that more of it is being scattered/absorbed. This result lead to the conclusion that the optimum thickness of the B:Si layer at a doping concentration of 5×10^{20} cm^{-3} is 10 μm. However, it is important to note that different doping concentrations will have different optimum thickness values. A result that was made clear in the simulations.

To confirm the experimental results of figure 11, a second set of three epiwafers were grown. These included the same B:Si epilayers as were used in the figure 11 structures, however an additional LOI, consisting of a 2 μm thick undoped i-Si epilayer, was now grown on top of each, completing the structure B epiwafer style defined previously. This was done to simulate the results that would be expected when measuring the thickness of a LOI using the proposed approach, and the FTIR characterisation of these is shown in figure 12. The reflection from the top and bottom of this new top layer creates what will be referred to hereafter as primary oscillations, which, as stated in section 1, are necessary for characterising the layer's thickness. However, it can be noted that as the thickness of the B:Si epilayer decreases, these oscillations become less defined. This is a result of reflection from the third interface, specifically the B:Si/Si wafer boundary, creating secondary oscillations that partially obscure the primary oscillations, and is why all light entering the B:Si epilayer must be scattered/absorbed to achieve the best results. As in figure 11, the epilayer with the 10 μm B:Si platform shows negligible evidence of interference from the B:Si/Si wafer boundary, and appears to give an ideal reflectance spectrum over the entire measurement range. An argument can also be made for the viability of the 6 μm thickness epiwafer, which has a small number of peaks without obvious interference effects. However, the limitation in peaks would increase the error on the modelled thickness when using automated software compared to data from a 10 μm thick epilayer, and so the accuracy of the result would be diminished. This interference is even more clearly pronounced in the epiwafer with a 2 μm B:Si platform, where interfering secondary oscillations are clearly visible in all but one of the primary oscillations. Therefore, results from this structure would have very large uncertainties. The

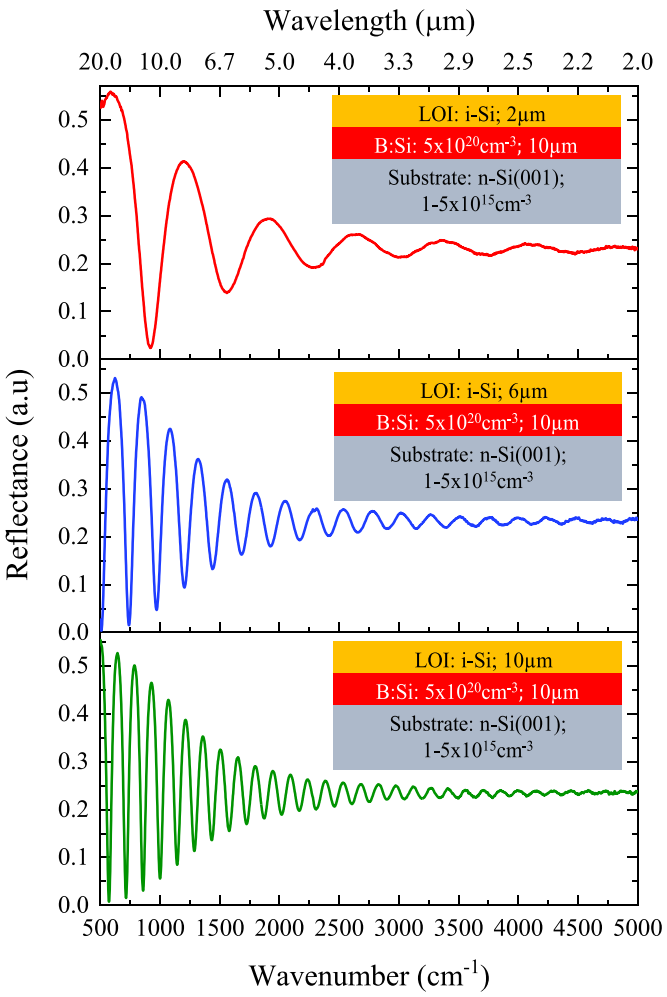

Figure 13. Reflectance spectra for undoped 2, 6 and 10 μm thick Si epilayers grown on a 5 $\times$ 10^{20} cm^{-3}, 10 μm thick B:Si platform. Reflectance data has been shifted to separate spectra for clarity.

figure 12 results clearly show that the proposed approach is viable for the thicker B:Si epilayers, and the recommendation for a thickness of 10 μm was upheld.

In the following series of results, and for the remaining results thereafter, B:Si epilayers with a B concentration of 5 $\times$ 10^{20} cm^{-3} and 10 μm thickness were utilised for the reasons described in the previous analysis. First, a series of undoped Si epilayers of varying thickness were grown on top of this B:Si platform, and used to evaluate the viability of the proposed approach for these different LOI thicknesses. The results of the subsequent FTIR characterisation on these three epiwafers are shown in figure 13.

Individually, each reflectance curve shows the same exponential decrease with increasing wavenumber, and all are also free of interference from the spectra of the B:Si epilayer itself (as would be expected from the previous analysis). When comparing the respective results to each other, however, distinctive variations in the oscillating frequency are observed. This oscillation frequency is proportional to the length of material through which the light has travelled before reaching the detector and is therefore also proportional to the thickness

Table 1. A comparison of three different epilayer thickness characterisation techniques: FTIR, spectroscopic ellipsometry (SE) and XRR.

	FTIR	Ellipsometry	XRR
Thickness range	∼500 nm–>100 μm	∼5–500 nm	∼10–150 nm
Measurement speed (seconds per data point)	∼5	∼5–∼2000	>2000
Spectrum analysis	Automatic, <10 s	Semi-automatic, >60 s	Semi-automatic, >60 s
200 mm wafer mapping with 100 points	<1 h	>1 h	>50 h

of the layer that is being characterised. This is because an increased path difference reduces the cycle period between constructive and destructive interference as wavelength is varied, and so the frequency increases. In addition to explaining the results of figure 13, this fact also places certain thickness constraints on a FTIR spectrometers thickness characterisation range. A lower bound is set because at least one oscillation period needs to be visible in the detected spectrum to make an accurate thickness measurement, and so any layer thinner than the corresponding thickness cannot be determined accurately. Conversely, at very high thicknesses the frequency can become too large, and the corresponding oscillation period too small, for the spectrometer to resolve, setting an upper bound. The specific upper and lower constraints therefore vary depending on the specific probe beam used and the resolution of the FTIR spectrometer, but a general range is given in table 1 for reference. The results of figure 13 clearly suggest that the proposed approach is suitable for characterising epilayer thicknesses across this range.

Another notable result of figure 13 is that the strength and clarity of the oscillations is greater than what was obtained using the traditional method, which can be seen by comparing the results of figure 12 to those of figure 3. This is because a wafers doping concentration are typically limited to a maximum of 5 $\times$ 10^{19} cm^{-3} by constraints associated with their production, whereas higher doping concentrations and doping uniformities have been shown to be achievable in the epitaxially grown B:Si epilayer. The higher doping concentration creates a sharper reflection boundary, resulting in a signal that is up to five times as strong. This increase in signal strength decreases the error on the thickness characterisation which, considering signal amplitude, oscillation frequency, and negligible secondary fringes, is estimated here to be ∼0.1%. The low uncertainty on the thickness measurements found with this approach supports its use as a replacement of the traditional approach.

To finalise the analysis of the proposed approach, two epiwafers were grown on to 200 mm diameter wafers at 1100 °C and subsequently compared. The first was in the same structure B style as the epiwafers analysed in figure 12, but with a

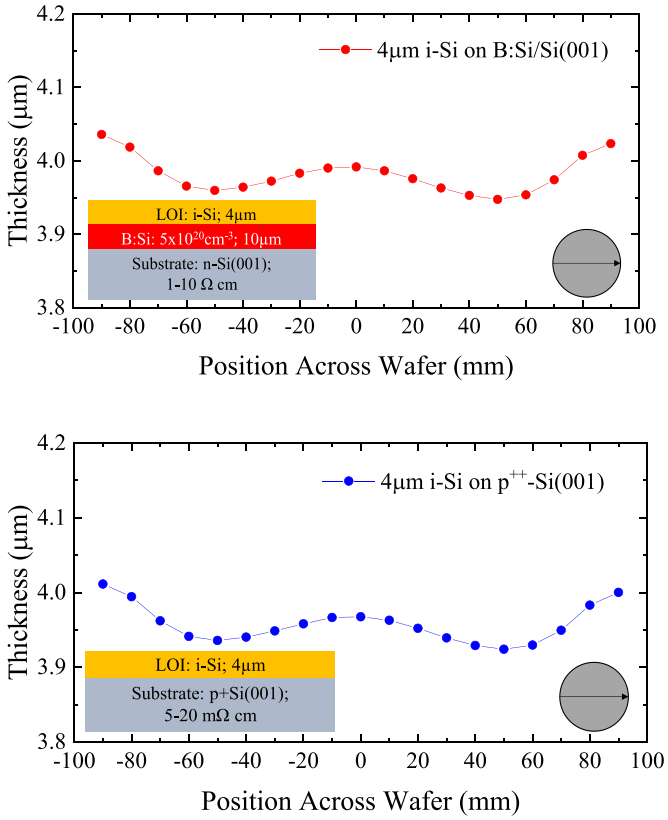

Figure 14. Thickness profiles across two 4 μm i-Si epilayers grown onto 200 mm diameter platforms, representing the proposed (top) and traditional (bottom) approaches respectively. The top figure shows thickness uniformity for the i-Si epilayer grown on the new B:Si/Si(001) epiwafer and the bottom one for the same i-Si epilayer grown on a traditional p^{++}-Si(001) wafer. The LOI thickness uniformity is 1.1% and σ/mean is 0.6%.

4 μm thick undoped Si LOI. In the second, an identical 4 μm thick undoped Si epilayer was also grown, but this time onto a heavily doped p^{++} Si(001) wafer platform. Thickness profiles of the two undoped Si epilayers are shown in figure 14. In these results, all slight thickness variations that exist between the two were found to be within the uncertainty of the FTIR measurement system, and in both cases the thickness uniformity was verified to remain approximately constant. The thickness uniformity of the structure B epiwafer was then also mapped using the FTIR technique and found to produce a uniformity of 1.15%, see figure 14. This indicates that, even with inclusion of the B:Si intermediary epilayer, the epiwafer can remain exceptionally uniform, validating the utility of this approach.

From the experimental data, it can be concluded that FTIR reflection spectroscopy can be performed on an undoped Si epilayer by including an intermediary layer of B:Si with an impurity concentration of 5×10^{20} cm^{-3} and a thickness of 10 μm. Using this combination of parameters, direct experimental evidence has been obtained that shows this method is capable of measuring LOI thicknesses above 2 μm to a similar or greater accuracy than the traditional approach, and extrapolating these results also suggests that it could be used to characterise Si epilayers down to the $\sim$0.5 μm thickness limit imposed by the single oscillation period requirement. Furthermore, this investigation has also found evidence that other parameter combinations could be used to obtain similar results. For example, the thickness of the B:Si epilayer could be decreased if the doping concentration is increased. This adds flexibility to the approach, allowing it to be tailored to a variety of specific situations.

A final note should be made regarding the decision to focus on verifying this approach for FTIR reflection spectroscopy over other optical reflection techniques, such as XRR and ellipsometry. The main reasons for this are outlined in table 1, which shows some of the significant advantages that FTIR reflection spectroscopy has over its alternatives. The first of these is its data acquisition speed, which was first mentioned in section 1. As a result of its reliance on only a single moving part, a Michelson–Morley interferometer which can be oscillated along its spatial length at high frequencies, a FTIR spectrometer can collect large quantities of data and make measurements faster than either ellipsometry or XRR. It is also easier to automate the process of data analysis using an FTIR spectrometer, allowing the final thickness to be determined quicker. Table 1 also highlights the superior thickness characterisation range of an FTIR spectrometer. Whereas the other two outlined techniques can only characterise thicknesses of under 0.5 μm, FTIR reflection spectroscopy can make accurate thickness measurements across a range of almost 100 μm [14]. This gives it a far broader range of applications that it can be applied to.

In addition to the advantages highlighted in table 1, further justification for the choice of FTIR reflection spectroscopy comes from its ability to acquire data across a wide spectrum, which gives it additional, more specific, advantages over monochromator techniques such as XRR [4]. The first is the multiplex gain (or Fellgate advantage). If the detector has N spectral elements of thickness $\Delta\lambda$, the FTIR spectrometer has a signal-to-noise ratio advantage of $N^{1/2}$ over monochromators limited by noise other than from photons. A second advantage is the Jacquinot advantage, where the lack of constraint on its aperture size means it has an optical throughput gain of approximately 100 when compared to monochromators.

For the reasons outlined above, it was concluded that an improved technique for FTIR reflection spectroscopy that removed the constraints of heavily doped wafers would have the broadest appeal. However, there are specific applications in which the other two techniques can be used more effectively. For example, both XRR and ellipsometry can measure the thickness of very thin epilayers, which is outside the characterisation range of FTIR reflection spectroscopy. Moreover, as both of these techniques also use reflection, they suffer from the same limitations imposed by heavily doped wafers. For this reason, it would be beneficial to follow up this investigation by adapting the approach outlined here to these two other techniques. Further investigation could also go to adapting this method to other semiconductor materials, such as Ge, GaN, GaAs and SiC [15–17], which compliment Si in the semiconductor industry.

6. Conclusion

In this work, a new approach to FTIR reflection spectroscopy has been proposed that utilises a 10 μm thick Si epilayer with a 5×10^{20} cm^{-3} doping concentration to create the reflection boundary necessary for thin film thickness characterisation. These specific parameters were found using a mixture of simulation and experiment; the simulations to provide theoretical guidance and constraints to the expected values, and the experimental work, which included the use of techniques such as 4PP, XRD, AFM and FTIR reflection spectroscopy, to fine tune and verify these. The results provide evidence that this structure would not only be a promising replacement to the traditional use of heavily doped wafers, but also suggest that it possesses additional, and initially unanticipated, advantages.

Using this B:Si epilayer structure, with B having been chosen specifically for its low diffusivity and segregation, it is possible to measure thicknesses across the full ~0.5–100 μm characterisation range that is available to FTIR reflection spectroscopy. More importantly though, the layer under analysis can be of any crystallographic orientation or off-cut. This removes the orientation constraint that was imposed by the limited commercial availability of heavily doped wafers, and was one of the main initial motivations behind this research. In addition to this, the very high doping concentration that is recommended for the B:Si epilayer, and that was proven to be possible for Si in this investigation, has been found to open up additional advantages for the proposed method over heavily doped wafers, which are constrained to a maximum concentration of 5×10^{20} cm^{-3}. First, the higher doping concentration was found to result in more accurate results, owing to the greater reflection boundary created at the B:Si/LOI interface increasing the strength of the detected oscillations by up to five times. Second, the higher doping concentration also means that the proposed technique can be used on epilayers with a variety of doping types and values. The traditional approach is far more limited in this regard, as even mild doping can alter the refractive index to align with the heavily doped wafer and diminish the reflection boundary. These latter advantages, although not anticipated initially, further support the viability of this method.

As well as providing experimental evidence in support of the use of a B:Si epilayer for FTIR spectroscopic analysis, this work has also opened avenues for further research specifically aimed at adapting this approach to a greater variety of applications. For example, this paper chose to focus on Si because of its pre-eminence in the semiconductor industry, but the approach could be adapted to other semiconductor materials such as Ge, GaN, GaAs and SiC and with relative ease. Furthermore, the most general aim of this research was to create an epitaxial platform that forms a reflection boundary between it and any subsequently grown layers. This is of course a key requirement of FTIR reflection spectroscopy, but other reflection techniques like XRR and ellipsometry also need this. If further research were to show that a reflection boundary was created within the relevant frequency ranges of these other techniques using the proposed structure, or that some other epilayer could be grown and provide such an interface, the general approach outlined in this investigation could be utilised as part of these techniques too. By combining the two generalisations discussed above, the approach to thickness characterisation proposed in this investigation could form an extremely adaptable and useful technique for future epilayer research.

Data availability statement

All data that support the findings of this study are included within the article (and any supplementary files).

Acknowledgment

This work was partially supported by the EPSRC.

ORCID iD

Maksym Myronov https://orcid.org/0000-0001-7757-2187

References

[1] Semiconductor Industry Association © 2021 Semiconductor Industry Association (available at: www.semiconductors.org) (Accessed 15 June 2021)
[2] Myronov M 2018 Chapter 3—molecular beam epitaxy of high mobility silicon, silicon germanium and germanium quantum well heterostructures *Molecular Beam Epitaxy* 2nd edn, ed M Henini (Amsterdam: Elsevier) pp 37–54
[3] Wilkes J G 1998 Silicon processing *Silicon Devices* ed K A Jackson
[4] Schroder D K 2006 *Semiconductor Material and Device Characterisation* 3rd edn (New York: Wiley)
[5] Airaksinen V M 2001 *Semiconductors and Semimetals* ed D Crippa, D L Rode and M Masi (Amsterdam: Elsevier) p 225
[6] Woo C, Sun Q and Yu T 2003 *Phil. Mag.* **83** 3753
[7] Ural A, Griffin P B and Plummer J D 1999 *J. Appl. Phys.* **85** 6440
[8] Colston G, Myronov M, Rhead S and Leadley D 2015 *Semicond. Sci. Technol.* **30** 114003
[9] Zhou Z H, Yang I, Yu F and Reif R 1993 *J. Appl. Phys.* **73** 7331
[10] Basu S, Lee B J and Zhang Z M 2009 *J. Heat Transfer* **132** 023302
[11] Adachi S 1989 *J. Appl. Phys.* **66** 3224
[12] Cutler M L 1939 Massachusetts Institute of Technology
[13] Bruker Optics VERTEX series FTIR spectrometer, (© 2018 Bruker Optics BOPT-4000046-06) (available at: www.bruker.com) (Accessed 29 December 2020)
[14] Quinten M 2012 Thin-film thickness determination *A Practical Guide to Optical Metrology for Thin Films* (Hoboken, NJ: Wiley) p 224
[15] Yoshida S, Hijikata Y and Yaguchi H 2012 *Physics and Technology of Silicon Carbide Devices* ed Y Hijikata (London: IntechOpen)
[16] Moellering R A, Bauer L B and Balestra C L 1990 *J. Electron. Mater.* **19** 181
[17] Horikiri F, Narita Y and Yoshida T 2017 *Jpn. J. Appl. Phys.* **56** 120301